IOP Conference Series: Materials Science and Engineering

PAPER • OPEN ACCESS

The effect of additive geometry on the integration of secondary elements during Friction Stir Processing

To cite this article: A Zens *et al* 2018 *IOP Conf. Ser.: Mater. Sci. Eng.* **373** 012018

View the article online for updates and enhancements.

Related content

- Microstructure and hardness performance of AA6061 aluminium composite using friction stir processing
  C D Marini and N Fatchurrohman

- Mechanical properties of Al-SiC Nano Composites fabricated by Friction Stir Processing
  A Arun Premnath, P. Likhil Varma, P. Sathya sai RamaKrishna et al.

- Microstructure Characterization of Al-TiC Surface Composite Fabricated by Friction Stir Processing
  Apireddi Shiva, Muralimohan Cheepu, Venkata Charan Kantumuchu et al.

The effect of additive geometry on the integration of secondary elements during Friction Stir Processing

A Zens[1,*], M Gnedel[2], M F Zaeh[1] and F Haider[2]

[1] Institute for Machine Tools and Industrial Management (*iwb*), Technical University of Munich, Boltzmannstr. 15, 85748 Garching, Germany
[2] Chair for Experimental Physics 1, University of Augsburg, Universitaetsstr. 1, 86159 Augsburg, Germany

[*] e-mail: amanda.zens@iwb.mw.tum.de

Abstract. Friction Stir Processing (FSP) can be used to locally modify properties in materials such as aluminium. This may be used, for example, to produce a fine microstructure or to integrate secondary elements into the base material. The purpose of this work is to examine the effect of the properties of the metal additives on the resulting material distribution in the processed region. For this, commercially pure iron and copper were integrated into an EN AW-1050 aluminium base material using FSP. Iron in the form of powder, wire and foil as well as copper in powder form were assessed. The various additive forms represent materials with differing surface-to-volume ratios as well as varying dispersion characteristics in the processing zone. The processing parameters for each additive form remained constant; however, two- and four-pass FSP processes were conducted. The results of CT analysis proved especially insightful regarding the spatial distribution of the various additive form within the workpiece. As expected, the powder additive was most widely distributed within the welding zone. Micro-hardness mappings showed that the powder additive contributed to the hardness within the weld nugget in comparison to the processed material without secondary elements.

1. Introduction and motivation

Friction Stir Processing (FSP) is an offshoot of Friction Stir Welding (FSW) and is used to create a locally refined microstructure in metal materials, most commonly aluminium. A schematic of the process, which is analogous to FSW, is shown in Figure 1a. First, a tool with rotational speed n, comprised of a shoulder and a probe, is plunged into the workpiece. During the plunge phase and processing, the material is softened due to the heat generated by friction between the workpiece and tool. After a short dwelling time, the tool is moved along the welding line at a feed rate v and with a force F_z. Once the process is complete, the tool is extracted. The microstructure of the area in which processing occurred can be divided into several zones (Figure 1b) [1]. In the nugget zone (NZ), through which the tool passes, intensive material deformation and dynamic recrystallization occurs. The microstructure here is characterized by very fine and homogeneous grains. In the directly adjacent thermo-mechanically affected zone (TMAZ), plastic deformation still occurs; however, grains are larger and aligned along a certain direction. In the heat-affected zone (HAZ), no deformation occurs, but the material is subject to elevated temperatures, which leads to enlarged grains compared to the

base material (BM). With regards to the material flow during FSP, a distinction must be made between the advancing side, in which the tangential velocity of the tool is in the same direction as the feed rate, and the retreating side, for which the opposite is true. It has been reported [2, 3] that the material flow in the nugget and the temperature around the nugget varies depending on which side is being considered; higher temperatures are reached on the advancing side compared to the retreating side.

FSP varies from FSW in that its primary purpose is not to weld two parts together, but rather to locally adapt the material properties. Mishra et al. [4] were the first to employ the FSP process in order to create surface composites by integrating an additive material (SiC) into the aluminium matrix in order to increase the surface hardness. Here, metal matrix composites (MMCs) were produced. Multi-pass welding is often necessary in order to assure a complete and homogeneous dispersion of the additive into the nugget. Various methods for depositing the additive material into the matrix via FSP can be found in literature. These include an application of the additive by spreading it over the material surface [4], inserting it into a groove machined out of the base material [5, 6], introducing it between plates in butt-weld configuration [7], and by integrating it in-situ via an adapted tool design [8]. Despite a variety of material deposition methods being reported, the form of the additive and its effect on the practicality of the process set-up and the resulting material properties has yet to be assessed.
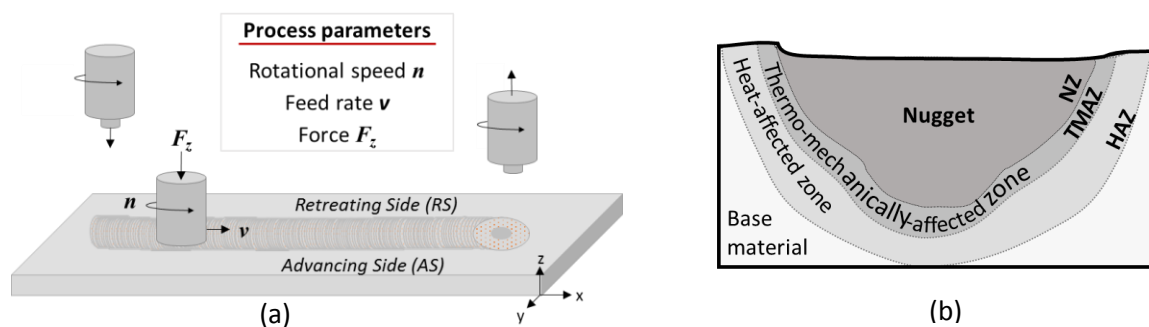

Figure 1. Schematic of the (a) FSP process and (b) areas of the process zone.

Researchers such as Hsu et al. [9] have reported using FSP to combine metal particles into the aluminium matrix in order to create MMCs. Here, the samples were first produced via powder metallurgy, which initiated the diffusion processes. Once multiple FSP passes were performed, it was reported that the additive material had completely reacted with the aluminium matrix to form Al-Cu intermetallic phases. This provided meaningful insights into the potential of FSP in order to process material via mechanical alloying; however, this method can only be applied to bulk materials: it cannot be used to locally change properties (i.e. chemical composition) in larger structures. The addition of copper to aluminium alloys via FSP is especially interesting because of the relatively high solubility of the Cu in Al and the potential to strengthen the material via the precipitation of secondary phases.

When powder is introduced as the additive material, the process is often referred to as Friction Powder Processing (FPP). Fujii et al. [7] performed FSP with iron powder additives in a 1050-H24 aluminium base and found that the mechanical properties of the material were enhanced by the formation of precipitates in the process zone. Abnar et al. [10] added copper powder to FSW welds of 3003 aluminium in order to counter the reduction in hardness and strength that typically occurs during FSW. They found that running the first and second passes in opposite directions (thus reversing the advancing and retreating sides) encouraged the creation of a homogeneous distribution of copper particles. In later works [11], the use of an aluminium-copper powder mixture was shown to improve the properties of the processing zone. Mahmoud and Tash [12] processed aluminium samples with additives of Fe and Fe_2O_3 powders in an aluminium matrix and analysed the magnetic properties.

The form of the additive is an important aspect to consider in designing a homogeneous processing zone and robust FSP process. The purpose of this work was to assess various aspects of the process set-up in order to integrate metal additives into an aluminium base using FSP. To begin, iron additives

with a range of geometries were processed into an aluminium matrix and the most suitable additive form was determined. Then, copper and iron additives were integrated into an aluminium base via FSP and compared with respect to their metallurgical and mechanical properties. Copper and iron were chosen due to their distinctly different solubility properties: copper has a relatively high solubility in aluminium, whereas iron is almost insoluble.

2. Experimental methods

2.1. Experimental set-up and materials

The base materials used in this work were sheets of 8 mm thick EN AW-1050 aluminium. Samples consisted of two 100 mm x 300 mm plates arranged in a butt-joint configuration. In order to insert the additive elements into the welding zone, a 1 mm wide groove was machined out of the (future) contact interface in one of the samples. The second plate was then placed over the additive-filled groove, thus containing the additive within the processing zone. The depth of the groove was dependent on the form of the additive. A schematic of the set-up can be found in Figure 2.

Experiments were performed on a Heller MCH 250 horizontal machining center. The employed tool consisted of a concave shoulder with diameter $d_s = 12$ mm as well as a probe with length $l_p = 3.5$ mm and diameter $d_p = 5$ mm. Temperature measurements were performed for selected trials. For this, K-type thermocouples with a diameter of 0.5 mm were placed into holes at various points along the welding line. The holes for the thermocouples were 0.6 mm in diameter and 2 mm deep. The locations of the thermocouples are given in Figure 2. The variation in employed materials and experimental set-up are as follows:
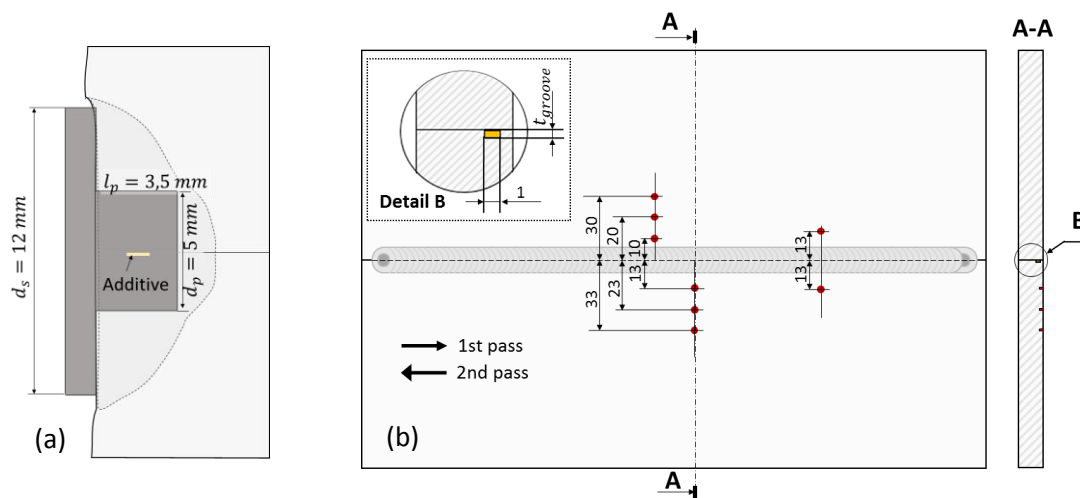

Figure 2. (a) Schematic of the probe geometry within the process zone and (b) schematic showing the location of the thermocouples.

2.1.1. Comparison of the additive geometry (Trial A)

Commercially pure iron in the form of powder, wire and foil was used as additive material. For foil and wire samples, a 50 µm deep groove was machined out of the aluminium sample ($t_{groove} = 50$ µm). Foil additives had a thickness of 50 µm and were cut to a width of 1 mm in order to fit into the groove. Several pieces of wire, each with a diameter of 50 µm, were placed into the groove until the amount iron present was comparable to experiments with foil additive. In order to assure a similar amount of iron in powder form (-200 mesh), the fill density was taken into account and the depth of the groove for powder additives was set to $t_{groove} = 130$ µm. Additives were located at a depth of 1.5 mm from the sample surface. The probe of the FSP-tool used in these experiments featured four flats machined at a 7° angle.

2.1.2. Comparison of iron and copper elements (Trial B)

Commercially pure iron and copper powders were used in order to compare the effect of the additive material on the properties of the processed zone. Iron powder with a size of -200 mesh and copper powder with diameter $d < 50$ μm were employed. The machined groove was 100 μm deep and was located at a distance of 1.0 mm from the sample surface. Additionally, a reference sample without additive material was processed for comparison. The probe of the FSP tool used in these experiments featured a screw profile with four flats machined at a 7° angle. The probe was rotated in a counterclockwise manner in order to drive the material into the processing zone and densify the material.

2.2. Processing parameters

The processing parameters remained constant for all experiments. The tool and additive were set up so that the additive was located at the center of the probe as it travelled through the processing zone. A rotational speed of $n = 1000$ rpm and feed rate of $v = 75$ mm/min were employed. The tool tilt angle was set to 2°. Experiments were run using position control with the plunge depth of 0.1 mm being held throughout the processing time. Samples from Trial A underwent a four-pass welding process with the feed rate direction being reversed for each pass. Samples from Trial B underwent two-pass processing with the second pass moving in the opposite direction of the first pass. The total weld line length was 265 mm.

2.3. Material characterization

The metallurgical and mechanical properties of the processed samples were characterized using a range of analysis methods. Computed tomography (CT) scans were performed in order to fully reconstruct and characterize the distribution of the additive elements throughout the processing zone. A voxel size of 5 μm was sufficient to get detailed information about the 3D shape of the intermixed material. Cross-sections at fixed positions revealed the spatial distribution in the given dimension. In order to assess the distribution of the additives within the processing zone, samples were ground and polished.

Samples from Trial B were etched using the Barker technique in order to increase the definition of the processing zone and to identify the dimensions of the nugget zone and the grain size. Also, hardness mappings with a spatial resolution of 300 μm in the x- and y-directions and a peak force of 0.5 N were carried out using a Berkovich nano-indenter in order to assess the influence of additive particles and grain structure on the hardness and to evaluate the potential dissolution of the additive metal into the aluminium matrix.

3. Results and discussion

3.1. Comparison of the initial additive geometry with iron components (Trial A)

The CT images, shown in Figure 3, provide information that cannot be extracted from optical images: most importantly, the distribution of the additive along the processing line. The extent of material distribution varied greatly depending on which additive type was used. For instance, the powder additive resulted in an hourglass shape and somewhat smeared appearance with various areas of clumping along the processing line. It is unclear whether the pattern of powder distribution along the welding line is a result of the probe profile or due to an inhomogeneous distribution during set-up. An explanation for this could be cold welding of the deposited powder before the tool reaches it; the heat transfer ahead of the tool, especially at relatively low welding speeds, may have cause particles to agglomerate or weld before the tool reached them. The powder may also have compacted while being deposited into the groove. Despite the inhomogeneous deposition along the welding line, the copper powder was the additive that was most widely distributed throughout the depth of the processing zone.

The original position of the wire additive was parallel to the feed direction, almost perpendicular to the position in which the wire is seen in the CT scans. During FSP, the wire was broken up and to a large extent aligned perpendicular to the tool path (tangent to the tool rotation direction). The wire pieces are located in a band about 1 mm from the aluminium surface in a width of about 1 mm, which correlates well with the 1 mm width of the machined groove in which it was originally placed. Hence, the wire was not distributed through the depth of the processing zone.

The trial with iron foil was more difficult to assess, as very few foil remnants were able to be found in the sample. Due to the very low solubility of iron in aluminium and the lack of dissolution of the powder and wire pieces within the aluminium matrix, it is highly unlikely that the foil was dissolved into the aluminium matrix. Rather, it is expected that the foil formed large clumps, which are located sporadically along the welding line. Composite images formed by overlapping all CT images of the xy-plane over the depth of the z-axis showed several areas with iron remnants.

Each additive geometry displayed various positive and negative aspects during the experimental set-up and the integration during FSP. For example, a powder additive has a comparatively high surface-to-volume ratio and thus would theoretically allow for a more rapid integration of additives into the matrix through diffusion processes. However, as powder sizes decrease, the handling of the powder becomes challenging as particles tend to clump together due to increased surface electrostatic forces. Additionally, bringing a specified amount of powder into a given area requires suitable application strategies and the amount deposited is essentially an estimation based on the measured fill density of the powder. A more practical option from an experimental set-up and a potential industrialization viewpoint it to use foil additives. Here, the amount of material given can be easily calculated and integrated into the processing zone using a machined groove or simply placing the material between two plates in a butt joint or overlap configuration. However, foils must first be torn apart and then distributed along the process zone during processing. The possibility to completely break apart and homogeneously distribute or dissolve foil additives is questionable. The additive in wire form was easy to deposit and the theoretical amount being integrated was relatively easy to calculate; however, the wire material did not spread throughout the depth of the processing zone as completely as the powder, and it remained present in the material as large pieces. Due to the larger scattering area of the powder within the processing zone, additives in powder form were selected for further analysis.
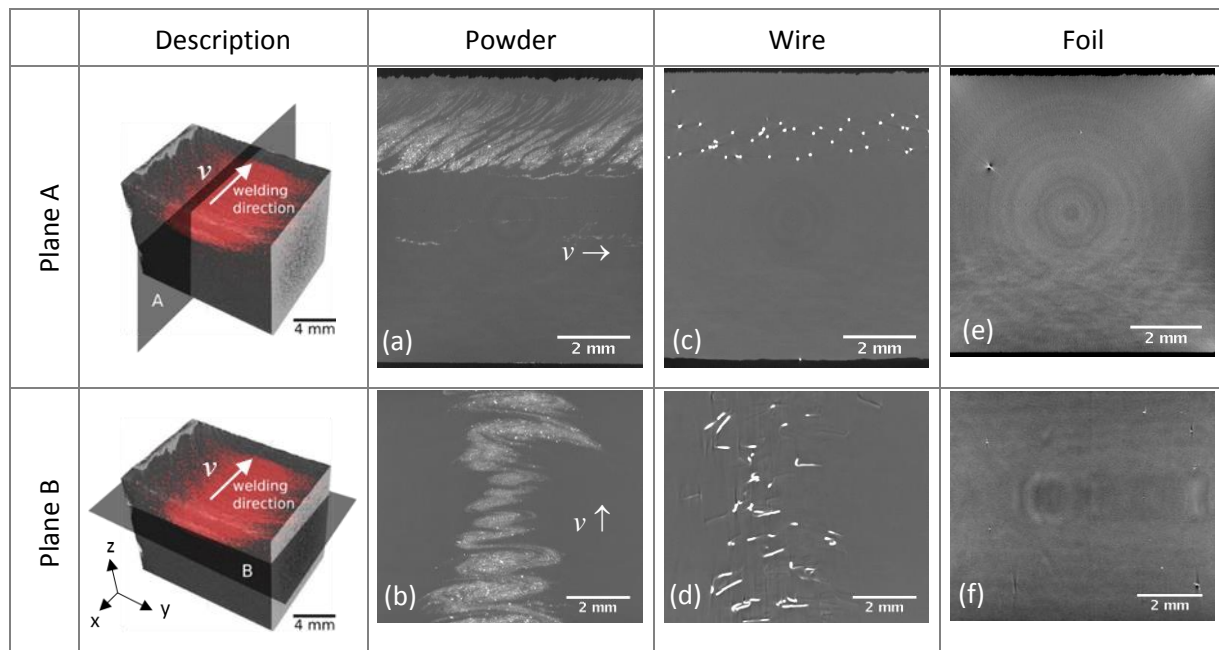

Figure 3. Cross sections taken from CT scans of aluminium (grey) with iron additives (white) in powder (a, b), wire (c, d) and foil (e, f) form. Images were taken from the xz-plane (plane A) and the xy-plane (plane B).

3.2. Comparison of iron and copper powder additives (Trial B)

A sample of the temperature measurements taken during the second pass of the FSP trial with iron powder additive can be seen in Figure 4. All trials yielded similar temperature profiles and the peak values varied only slightly, as demonstrated by the plot of the maximum temperature for each acquired data set (Figure 5).

As seen in Figure 5, the maximum temperature at a distance of 10 mm from the weld center (4 mm from the edge of the tool shoulder) ranged from 290-294 °C. Given the steep, nonlinear trend towards rising temperatures when moving closer to the process zone, it is expected that the temperature in the nugget zone was higher than the recorded temperatures. Increasing the rotational speed would also presumably increase the temperature and accelerate the diffusion processes.

There was no discernable difference in temperatures between the advancing and retreating side; however, the measurements taken from points 1 and 5 were systematically lower than those taken at point 2, although they were at the same distance from the center line. The reason for this may be the difference in proximity to the edge of the workpiece. Due to technical problems which occurred during processing, some measurement points were not able to be recorded (i.e. point 4 for the experiment with copper additives). Figure 5 shows that the thermal cycles for samples with iron and copper were very similar.
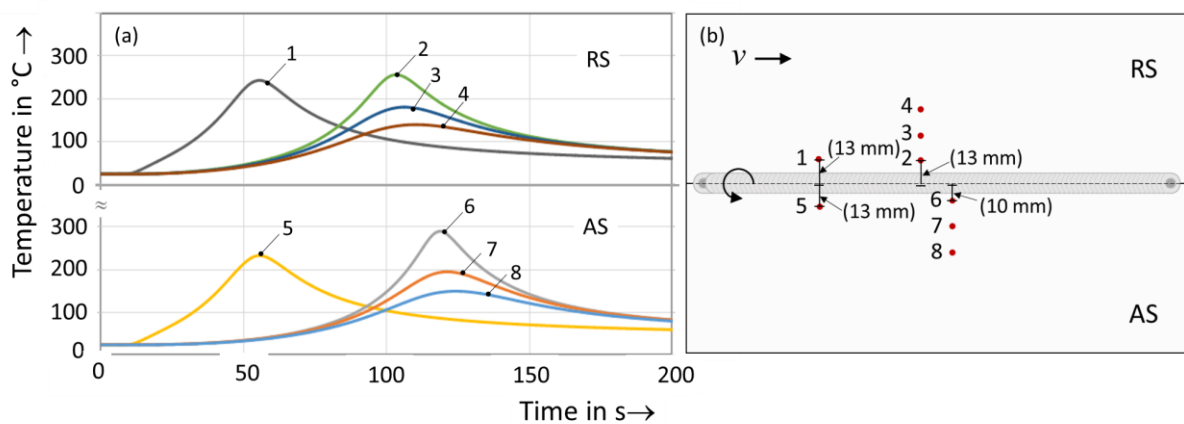

Figure 4. Temperature curves taken during FSP processing (a) and a schematic (b) showing the positions of the thermocouples. The numbering of the curves shows the thermocouple positions.
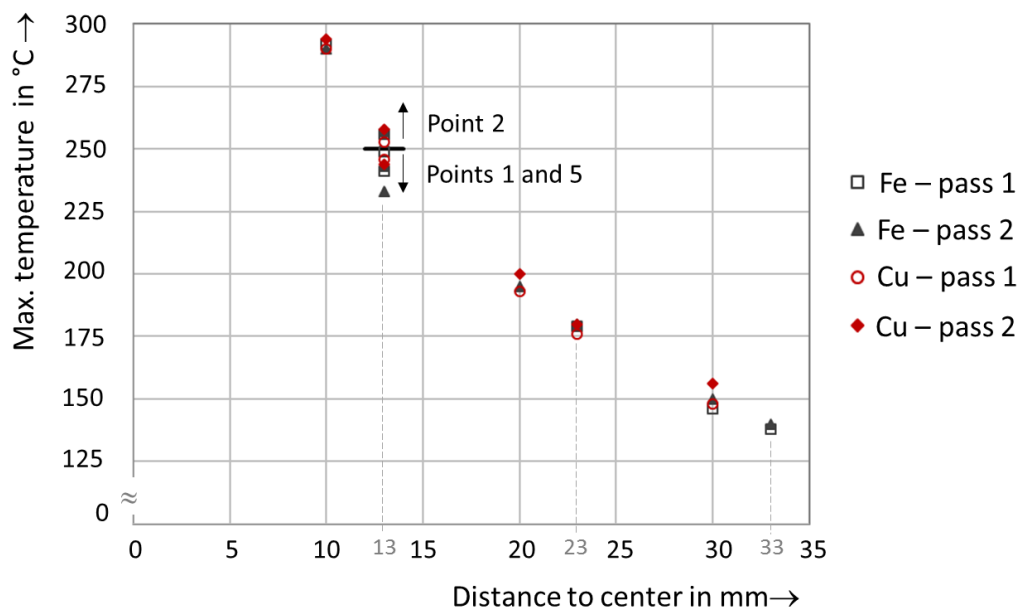

Figure 5. Plot of the maximum temperature for each thermocouple.

Regarding the grain structure, no significant differences between the trials with additives and the reference trial could be found (Figure 6). A higher influence of the additive metal on the dynamic recrystallization behavior during FSP is expected when the amount of additive is increased and when it is more homogeneously distributed. Within stir zone, no individual grains are visible due to lack of resolution. A significant difference in the advancing side (AS) and retreating side (RS) of the second pass was not observed; both sides appear to be symmetric in terms of grain size.
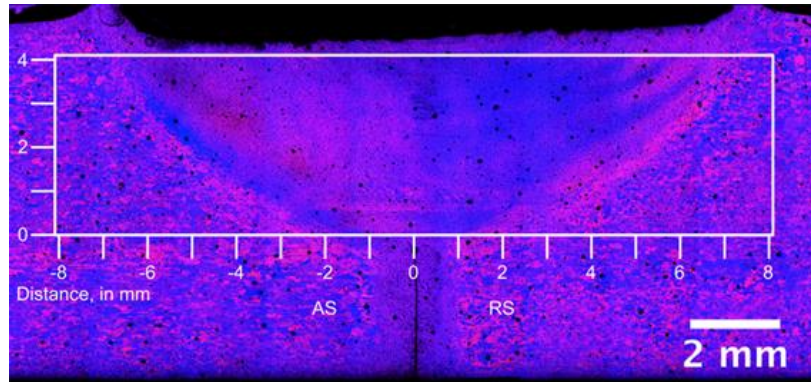

Figure 6. A cross section of the reference sample showing the difference in grain size between the nugget and base material. The sample was taken in the welding direction (AS and RS refer to second pass) and color-etched using the Barker-technique. The area use for hardness mappings, shown in Figure 7, is indicated.

The hardness mappings shown in Figure 7 indicate hardness up to 48 HV in the area where the copper powder was originally placed, which is up to 10 HV more than the corresponding area in on the reference sample. The iron particles led to a hardness of around 40 HV in this area. The main reason for the high peak hardness values in the area of the additive particles may have several factors; for one, intermetallic multilayers between the particles and the aluminium matrix are formed during the process, which typically exhibit substantially higher hardnesses than the base metals. An additional factor is the distribution of the powder within the nugget; if the additive material clumped in the area of the groove, rather than being distributed throughout the nugget, it would also lead to a rise in hardness.
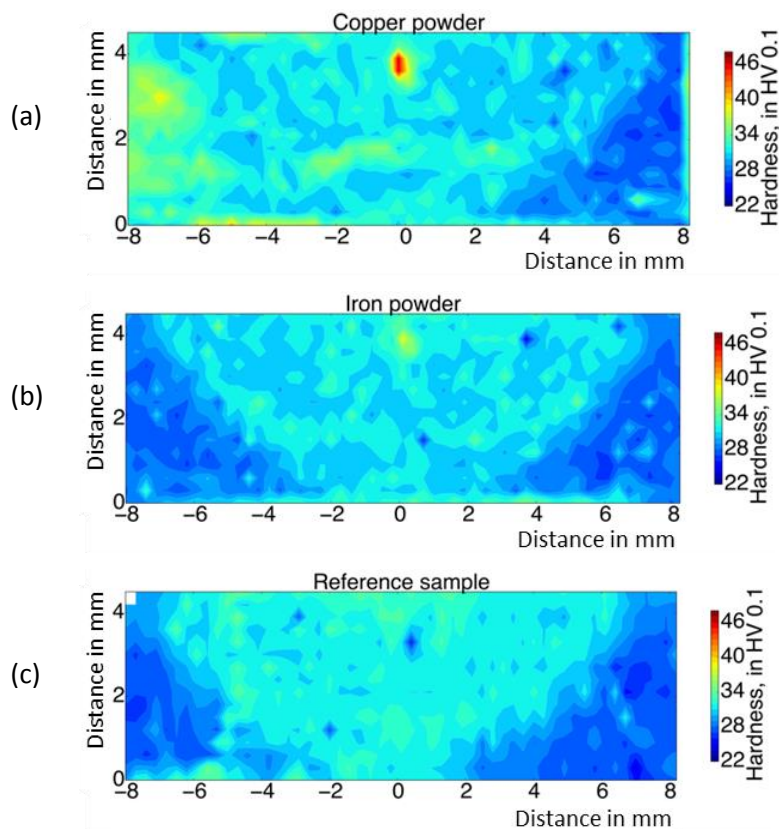
Figure 7. Hardness mappings with a resolution of 300 x 300 μm carried out with a Berkovich indenter of the cross section in welding direction of EN-AW 1050 with (a) copper particles, (b) iron particles, and (c) without additive particles.

Apart from the influence of the additive particles, the hardness maps reflect the grain structure in Figure 6 to the extent that the micrometer-sized dynamically recrystallized grains in the stir zone (nugget) lead to an increase in hardness of up to 10 HV. The hardness profile of the reference sample and the sample with iron powder appeared to be relatively symmetric within the processing zone; however, higher hardness values were found on the AS of the sample with copper powder, outside of the nugget zone. This occurrence cannot be explained in the framework of this paper.

4. Summary and outlook
In this work, the effect of the additive material and geometry in the creation of MMCs using FSP was assessed. Commercially pure iron additives in powder, wire, and foil form were integrated into an aluminium matrix using FSP. Foil and wire additives proved easy to deposit and also offered an easy way to control how much material was being added. However, based on the distribution and greater potential for powder additives to dissolve into the matrix, they were selected as the most suitable for the FSP process and were selected for further processing. Next, copper and iron additives in powder form were processed into the aluminium sheets. The hardness of the powder samples in the area of additive deposition was higher than the reference sample by about 10 HV. Despite these improvements, more suitable parameters must be found to deposit the powder material throughout the nugget and create a more homogeneous processing zone.

5. References

[1] Mishra R S and Mahoney M W (eds) 2007 *Friction Stir Welding and Processing* (Materials Park, Ohio: ASM International)

[2] Nandan R, Roy G G, Lienert T J and Debroy T 2007 Three-dimensional heat and material flow during friction stir welding of mild steel *Acta Materialia* **55** 883–95

[3] Shercliff H R and Colegrove P A 2007 Process Modeling *Friction Stir Welding and Processing* ed R S Mishra and M W Mahoney (Materials Park, Ohio: ASM International) 187–217

[4] Mishra RS, Ma ZY and Charit I 2003 Friction stir processing: A novel technique for fabrication of surface composite *Materials Science and Engineering: A* **341** 307–10

[5] Gandra J, Miranda R, Vilaça P, Velhinho A and Teixeira J P 2011 Functionally graded materials produced by friction stir processing *Journal of Materials Processing Technology* **211** 1659–68

[6] Lee C J, Huang J C and Hsieh P J 2006 Mg based nano-composites fabricated by friction stir processing *Scripta Materialia* **54** 1415–20

[7] Fujii H, Sun Y, Inada K, Ji Y, Yokoyama Y, Kimura H and Inoue A 2011 Fabrication of Fe-Based Metallic Glass Particle Reinforced Al-Based Composite Materials by Friction Stir Processing *Mater. Trans.* **52** 1634–40

[8] Huang Y, Wang T, Guo W, Wan L and Lv S 2014 Microstructure and surface mechanical property of AZ31 Mg/SiCp surface composite fabricated by Direct Friction Stir Processing *Materials & Design* **59** 274–8

[9] Hsu C J, Kao P W and Ho N J 2007 Intermetallic-reinforced aluminium matrix composites produced in situ by friction stir processing *Materials Letters* **61** 1315–8

[10] Abnar B, Kazeminezhad M and Kokabi A H 2014 The Effect of Cu Powder During Friction Stir Welding on Microstructure and Mechanical Properties of AA3003-H18 *Metall and Mat Trans A* **45** 3882–91

[11] Abnar B, Kazeminezhad M and Kokabi A H 2015 The Effect of Premixed Al-Cu Powder on the Stir Zone in Friction Stir Welding of AA3003-H18 *J. of Materi Eng and Perform* **24** 1086–93

[12] Mahmoud E R I and Tash M M 2016 Characterization of Aluminium-Based-Surface Matrix Composites with Iron and Iron Oxide Fabricated by Friction Stir Processing *Materials (Basel, Switzerland)* **9**